Published in final edited form as:
Mol Imaging. 2010 August ; 9(4): 192–200.

Quantitative analysis of HER2 receptors expression *in vivo* by NIR optical imaging

Victor Chernomordik[1,*], **Moinuddin Hassan**[1,*], **Sang Bong Lee**[2,3], **Rafal Zielinski**[2], **Amir Gandjbakhche**[1], and **Jacek Capala**[2]

[1]Program in Physical Biology, Lab. of Integrative and Medical Biophysics,National Institute of Child Health and Human Development, National Institutes of Health, Bethesda, Maryland, USA

[2]Radiation Oncology Branch, National Cancer Institute, National Institutes of Health (NIH), Bethesda, Maryland, USA

Abstract

Human epidermal growth factor receptor 2 (HER2) overexpression in breast cancers is associated with poor prognosis and resistance to therapy. Current techniques for estimating this important characteristic use *ex vivo* assays that require tissue biopsies. We suggest a novel noninvasive method to characterize HER2 expression *in vivo*, using optical imaging, based on HER2-specific probes (albumin-binding domain-fused-$(Z_{HER2:342})_2$ Affibody molecules, labeled with AlexaFluor750) that could be used concomitantly with HER2-targeted therapy. Subcutaneous tumor xenografts, expressing different levels of HER2, were imaged with a NIR fluorescence small-animal imaging system at several times post-injection of the probe. The compartmental ligands-receptor model was used to calculate HER2 expression from imaging data. Correlation between tumor cells HER2 amplification/overexpression and parameters, directly estimated from the sequence of optical images is observed (e.g., experimental data for BT474 xenografts indicate that initial slope, characterizing the temporal dependence of the fluorescence intensity detected in the tumor, linearly depends on the HER2 expression, as measured *ex vivo* by an ELISA assay for the same tumor). Results obtained from tumors expressing different levels of HER2 substantiate a similar relationship between the initial slope and HER2 amplification/overexpression. This work shows that optical imaging, combined with mathematical modeling, allows noninvasive monitoring of HER2 expression *in vivo*.

Keywords

Breast cancer; HER2 receptors quantification; Fluorescence Imaging; Affibody

INTRODUCTION

Advances in tumor biology created a foundation for targeted therapy aimed at inactivation of specific molecular mechanisms responsible for malignant transformation, supporting uncontrolled growth, and interfering with conventional therapies. In recent years, application of monoclonal antibodies (mAb) has become more and more attractive as a therapeutic modality of choice for malignancies expressing tumor-specific surface receptors[1]. The most prominent example of this approach is use of trastuzumab for treatment of HER2-positive

Corresponding author: Amir H Gandjbakhche, National Institutes of Health, 9 Memorial Drive, Bethesda, MD 20892, USA. Phone: 301-435-9235, Fax 301-480-2427, amir@helix.nih.gov.
[3]Current affiliation: Food and Drug Administration, Bethesda, Maryland, USA
[*]**Author Contributions:** V. Chernomordik and M. Hassan contributed equally to this work.

breast cancer[1,2]. Since the efficacy of this HER2-specific antibody depends on the overexpression of its target on tumor cells[3], patients' selection should be based on the HER2 expression level, not only on the bulk of the tumor, but also on the metastatic lesions that might not be amiable for biopsy. Therefore, development of imaging techniques enabling global assessment of receptor expression has become extremely important for proper diagnosis and selection of appropriate therapy for each individual patient. Limited invasiveness of such techniques would also allow optimizing of the treatment schedule and early monitoring of the response to the therapy by assessment of the changes in receptor expression over the course of treatment.

Radiolabeled trastuzumab [4–7], or F(ab′) fragments of trastuzumab have been used for imaging of HER2-positive tumors. However, due to the competition of the imaging and therapeutic molecules for binding to these receptors, trastuzumab-based tracers cannot be used to monitor possible changes in HER2 expression caused by treatment with this antibody. A promising alternative to antibodies as targeting agents is the use of Affibody molecules[8,9]. These relatively stable proteins are not only smaller than single-chain antibody fragments and, therefore, require a shorter washout time for an optimal signal-to-background ratio, but also bind to a different HER2 epitope than trastuzumab. Not interfering with trastuzumab, affibody molecules may be used to monitor HER2 expression changes in tumors treated with this antibody. We and others have described radioconjugates of Affibody molecules labeled with In-111[10], Tc-99m[9], F-18 [11,12] and Alexa Fluor [8].

Due to its minimal invasiveness, optical imaging presents an attractive option for serial imaging of tumors and monitoring of possible changes of receptor expression during the course of treatment. Reduced fluorescence background and enhanced tissue penetration by near-infrared (NIR) light allows detection of targets located at the depth of several centimeters in the tissues[13,14]. Over the past years, many groups reported successful *in vivo* NIR fluorescence imaging[15–19]. Although most of these studies are qualitative, quantitative methods necessary for adequate monitoring of the receptor status are beginning to emerge [8,20].

In this work we investigated whether temporal changes of the signal detected in tumor xenografts following injection of an Affibody-based, HER2-specific fluorescence contrast agent could be used to monitor the *in vivo* status of the receptors.

Materials and Methods

Imaging Probe

Labeling of HER2-specific ABD-$(Z_{HER2:342})_2$-Cys Affibody molecules (Affibody AB, Solna, Sweden) with Alexa Fluor 750 fluorophores (Molecular probe, Invitrogen, CA, USA) and the *in vitro* and *in vivo* characteristics of the resulting conjugate have been described in detail in our previous report[8].

Tumor Models

The animal study has been approved by the Institutional Review Board of the National Cancer Institute (Animal Study Proposal # ROB-117). The total number of animals used was 21. Tumor cells (BT474, MD-MBA-361, MCF7 and U251) expressing different levels of HER2 were implanted into the right flanks of 6- to 8-week-old athymic nude mice as described before[8]. Briefly, 5–10 × 10^6 cells in 0.2 mL of 50% Matrigel (BD Biosciences, Bedford, MA) were injected subcutaneously into the right flanks. Using calipers, tumor size was measured periodically and the tumors were allowed to grow to approximately 5 mm in diameter. Typical weight of the xenografts used for the imaging study was 100–300 mg. In the initial set of experiments, we considered three mice in each tumor category (the only

exception was the U251 case, i.e., the tumor with no HER 2 receptors, where data from one mouse were analyzed). The follow-up measurements, aimed at comparison of post-injection temporal variations of the fluorescence intensity in the tumor area with HER2 overexpression as measured in the same tumor by conventional ELISA assay *ex vivo*, were performed for a sample of 5 mice with xenografts of BT474 carcinoma, expressing the highest level of HER2 (3+).

Fluorescent Measurements

Fluorescence intensity was quantified using an in-house-created, time-resolved NIR fluorescence small-animal imaging system[20], operating in reflection geometry. This system includes a time-correlated single–photon counting device (SPC-730, Becker & Hickl, Berlin, Germany) in conjunction with a high repetition-rate tunable pulse laser (Tsunami, Spectra Physics, Mountain View, CA, USA) to detect individual photons. It uses a photomultiplier tube (PMT) (R7422, Hamamatsu Corporation, Hamamatsu City, Japan) as a detector, and a temperature-controlled scanning stage (National Aperture, Inc., NH, USA) with an electrocardiogram and temperature monitoring device (Indus Instrument, TX, USA). The imaging head of the device incorporates multimode optical fibers, delivering light from an excitation source to the sample and emitted fluorescence signal from the sample to the detector. The fibers were arranged as a linear array with one of the end fibers, coupled to the excitation laser beam, being used as a source fiber, while other fibers were used to collect emitted (fluorescent) light. To measure time-resolved fluorescence intensity, emitted light was delivered to the PMT via detection fibers. The small animal imager scanned the sample surface (e.g., skin or other tissue) in a raster pattern, producing a real-time 2D image. A cooled CCD camera was located on the top of the scanning stage to guide the scan to the region of interest (ROI). In the current study, a laser source of 750 nm was used to excite the fluorophore, and an emission filter of 780 nm was used for fluorescence detection. Our approach does not involve 3-D reconstruction of the tissue abnormality, as implied by conventional optical tomography. Instead we use reflectance imaging of the region of interest to realize a novel tool for optical biopsy. This methodology allows us to quantify the tumor cells' characteristics *in vivo* from the time sequence of fluorescent images.

To analyze the specific target accumulation of the imaging probes, mice were anesthetized by inhalation of isoflurane. Approximately 10 micrograms of Affibody conjugates were injected into the tail vein and imaged at predetermined time points after injection. The fluorescence signal mean and standard deviation were calculated by averaging the maximum pixel values over the tumor area and corresponding contralateral site. In the initial series of experiments, aimed at quantification of the time courses of fluorescence intensities for different types of carcinomas, measurements started 3 hours after injection and were performed during 72–75 hours after injection (at 8 time points t_i = 3, 6, 12, 20, 24, 30, 48, 72 hours for BT474; t_i = 3, 6, 10, 18, 21, 26, 48, 75 hours for MD-MBA-361; t_i = 3, 6, 12, 21, 24, 28, 48, 72 hours for MCF7). In the follow-up series, focused on analysis of individual variations in HER2 expression for the same type of tumor (BT474), two time points were added to the measurement sequence to investigate more accurately the initial rise in the fluorescence intensity after injection of the contrast agent (t_0 = 1–2 hours and t_4 = 13–14 hours).

Enzyme-linked immunosorbent assay (ELISA)—To determine HER2 protein level in cell lines of the tumor, an ELISA test was performed. *Ex vivo* tumor tissue was homogenized in a suspension buffer supplemented with a proteases inhibitor mix (Complete stop, Roche) and EDTA (5 mM), followed by HER2 extraction and centrifugation. An HER2 ELISA assay was performed according to the protocol provided by the manufacturer

(Calbiochem, Gibbstown, NJ) using a serial dilution of recombinant HER2 protein as standards. HER2 concentration is expressed in ng of HER2 per mg of total protein.

Mathematical Model

Theoretical analysis of the data is based on the compartmental ligand-receptor model, a simpler version of the one used for quantification of the specific receptor density in PET studies[21]. The non-equilibrium, nonlinear model includes three compartments (free ligand in blood plasma, free ligand in tissue, and, specifically HER2 receptor-bound ligand with concentrations C_a^*, F^*, and B^*, respectively). Association of fluorescent ligands (affibodies) with HER2 receptors is determined by the kinetic rate k_{on}. The total concentration of available HER2 receptors in the tumor, $B'_{\max}$, limits the binding process.

Several assumptions were made in this study to simplify our analysis. 1) The dissociation rate constant is low enough to disregard the ligands-receptor dissociation during the whole observation period of 0 to 72–75 hours. 2) The end of the initial distribution phase, when free ligands are uniformly distributed in the mouse blood stream, occurs before t_1 = 3 h. 3) The HER2-receptor-bound ligands' concentration in the tumor area B^* is negligible at $t = t_1$. 4). Local free ligands concentration in the tumor tissue $F^*(t)$ is constant during the measurement period, $t \geq t_1$. Applicability of these assumptions for our case is substantiated by analysis of the experimental data in Section 3. To avoid potential misunderstanding, it is worth noting that characteristic timescales for specific accumulation of the contrast agent in the tumor area are expected to be much longer in the case of conjugates of Alexa Fluor 750 with an albumin-binding domain (ABD)-congaing Affibody used in this study, as compared to those observed for HER2-specific Affibody conjugates used in PET imaging studies.

At the first approximation, accumulation of the HER2-bound fluorescent-labeled Affibody molecules in the tumor is described by a simple equation:

$$\begin{gathered}\frac{dB^*(t)}{dt} = k_{on}(B'_{\max} - B^*(t))F^*(t) \\ B^*(0) = 0,\end{gathered} \tag{1}$$

similar to Equation 6A from the paper by Delforge et al. [21].

Thus, for F^* = const:

$$B^*(t) = B'_{\max}[1 - \exp(-k_{on} t F^*)] \tag{2}$$

If the fluorescence intensity, as a function of time, is measured over a relatively long period of time up to $t > 1/k_{on}F^*$, Equation (2) is a good starting point to quantify $B'_{\max}$, although, if k_{on} or F^* is not known; only relative values of $B'_{\max}$ for different tumor types can be found.

Fluorescent intensity, originating from the tumor area, consists of three major components, related to free ligands in blood and tumor tissue, and ligands bound to HER2 receptors, respectively:

$$I_f = I_{bl} + I_{F^*} + I_{B^*} = \alpha C_a^*(0)\exp(-\frac{t}{\tau}) + \gamma F^* + \varepsilon B'_{\max}[1 - \exp(-k_{on} t F^*)], \tag{3}$$

Where coefficients α, γ and ε are assumed constant, decay time τ is to be determined from contralateral measurements, and the initial concentration of bound ligands (the last term) is zero. We suggest that concentration of free ligands in tumor tissue F^* = const for $t \geq t_1$ (i.e.,

after the initial distribution phase). Hence, the natural steps to separate their contributions are: 1) Normalize intensity data for all mice to the same initial level, corresponding to some early time point, say the average value of $I_0/_{t=3\ \mathrm{h}}$, measured for the BT474 sub-sample. 2) Exclude the effect of free ligands in blood plasma from measured intensities by subtracting values of $I_{bl}(t) = I(t_1)\exp[-(t - t_1)/\tau]$ from the measured intensities for the whole time series of the experiment. 3) Fit obtained data points with the function $y(t) = y_0 + a[1 - \exp(-bt)]$,considering y_0, a, and b, as fitting parameters, and using a standard curve fitting routine, e.g., a non-linear regression tool from SigmaPlot 9, 11 (Systat Software, CA, USA). Information about the relative value of $B'_{\max}$ can be derived either from the product of $P=ab=\varepsilon k_{on} F^* B'_{\max} \propto B'_{\max}$, or $S = y_0 + a$, ie, initial slope of dependence, or asymptotic value of $I_F^* + I_B^*(t)$ dependence. The latter, according to Equation 3, should be a linear function of $B'_{\max}$, i.e., $S=\gamma F^*+\varepsilon B'_{\max}$.

Results

Considerable changes in fluorescence intensity over time were observed. While significant variations in the temporal course of fluorescent intensity from the tumor were apparently correlated with the tumor type, the temporal data from the contralateral site were similar for all cases, reflecting approximately exponential decrease of the free ligands concentration in the blood, resulting, likely, from the washout of the fluorophores due to blood circulation, accompanied by degradation of the fluorescent ligands in the mouse kidneys.. In Figure 1a we present corresponding exponential fits $I_{bl}(t) = I_{bl}(0)\exp(-\lambda t)$ for MCF7 and MDA-MB361 temporal profiles of fluorescence intensity. Data after the background subtraction have been averaged over the corresponding samples. It should be noted that the washout time, $\tau = 1/\lambda \approx 27$ hours in both cases. Similar values of washout time also characterize other tumor categories. The case of the U251 tumor is of special interest, because the absence of HER2 receptors in the cancer cells indicates that temporal profiles of the fluorescence intensities from the tumor and the contralateral site are likely to be similar. As can be seen from Figure 1b, observations substantiate this conclusion: although the fluorescent image of the tumor is much brighter than that of the contralateral site, both the tumor data in the range 3 h ≤ t ≤ 24 h, as well as contralateral data for 3 h < t ≤ 72 h can be fitted by a similar exponential decay law:

$$I_{bl}^{um,con}(t)=I_{bl}^{um,con}(0)\exp(-\frac{t}{\tau}) \quad (4)$$

Here the exponential decay time is similar, τ = 27–28 h for the two sites. Higher tumor intensities can be explained by the higher blood volume compared to normal tissue, resulting from angiogenesis. For $t \geq 30$ h, tumor data imply an additional contribution to fluorescence intensity from some other (that is, other than blood) ligands compartment, e.g., free ligands in tissue. This potential contribution slowly increases with time (from 5140 to 5828 units between t = 48 h and t = 75 h).

For analysis of HER2 receptor concentration, we use the temporal variation of the difference between signal from the tumor area and that of the contralateral side. This allows us to eliminate the background and, partly, the contribution from the free ligands in blood. A special procedure to exclude additional blood contribution, resulting from increased blood volume in the tumor area, is described in the next section.

Imaging data from the tumor area, taken at some arbitrary time point after injection, may seem similar for different types of tumors. All of them present a bright spot close to the tumor center. However, a close look at corresponding temporal dependencies of the

fluorescent intensity reveals important qualitative differences in these profiles for tumors with different levels of HER2 expression. This fact is illustrated by Figure 2a, where the difference between the signal from the tumor and that of the contralateral side is presented as a function of time for four tumor types, differing in HER2 expression. All the data have been normalized on an initial time point (3 hours). One can see that there is a clear maximum in this intensity dependence for carcinomas with overexpressed HER2, and it is most prominent for BT474 tumor that has the highest expression level of HER2. On the other hand, for U251 tumor with no HER2 overexpression, this intensity just decreases with time.

To substantiate our assumption that most of the specific probe accumulation at the tumor occurs after t_1 = 3 h, even for the BT474 carcinoma, expressing the highest level of HER2, we present in Figure 2b a typical dependence of the difference between signal from the tumor area and that of the contralateral side, measured for one of the mice in the second series of measurements, when the data for shorter times, t_0 = 1 h, are available. The obtained curve presents a steep rise in fluorescence intensity up to the maximum value, reached at t ~20h.

In the Table 1, we present temporal data (tumor minus contralateral side), averaged over all tumor category sub-samples that are the basis for our further investigation.

We used the simple kinetics model, as described above, to estimate relative concentrations of HER2 receptors for three types of tumors from the data in Table 1 (tumor minus contralateral side), averaged over each tumor category subsample. Since it is complicated to control the initial concentration of labeled Affibody molecules in the blood circulation, due to different total blood volume in the mouse circulation and inaccuracies in preparation of marker solution for injection, it is reasonable to start with normalization of intensity data for all mice at the same initial level, say the average value of $I_0/_{t=3\ \mathrm{h}}$, measured for the BT474 subsample. Then, we subtracted the free ligands in the blood component (making the initial intensity value equal to 0) and fit the data to the model.

In Figure 3 the results of this procedure are presented for BT474, MDA-MB361, and MCF7 xenografts. Obtained parameters of initial slope $P = ab$ and asymptotic intensity $S = y_0 + a$, which are presented in Table 2, were compared with known parameters from the literature data on amplification and overexpression of HER2 in breast carcinoma cell lines (see the values published in Pegram et al.[22] and Kallioniemi et al.[23]).

The correlation found between tumor cell characteristics and parameters, directly estimated from the optical images, is shown in Figure 4a, b and 5. Three plots in Figure 4a illustrate the observed correlation of the slope P with HER-2/neu expression (I), HER2 gene copy per cell (II), HER2 gene copy per 17cen (III), and columns 2, 3 and 4 from Table 1 of [22] (columns 3 and 4 are obtained by the fluorescent in situ hybridization method [8]). Which of these intrinsic parameters better describes the concentration of HER2 *in vivo*, $B'_{\max}$, is not clear at this point. However, one can see that over the broad range of HER2 characteristics, all these plots are well represented by linear regression, passing through the origin, as expected from Equation 2, although larger deviations from linearity are observed for HER-2/neu expression.

Similar results are observed for the asymptotic parameter S (Figure 4b): linear dependencies on the above-mentioned tumor HER2 characteristics, I, II, III, although not passing through the origin ($S \neq 0$ for $B'_{\max} = 0$, implied by zero value of I, II, and III), possibly due to the contribution of unlabeled Affibody molecules in the tumor tissue (second term in the LHS of Equation 4). It is worth noting that, according to linear regression fit, the residual intensity for $B'_{\max} = 0$ is $I_r \approx 5600 \pm 250$ a. u, which is close to the residual intensity of ~5800 a. u.,

observed at t =72 h. for the case of tumor U251 without HER2 receptors (after subtraction of blood contribution). Parameters are summarized in Table 3.

To further substantiate our methodology and to improve its statistical significance, in the follow-up experiments we compared post-injection temporal variations of the fluorescence intensity in the tumor area with individual HER2 overexpression, measured *ex vivo* in the same tumor by conventional ELISA. This analysis was performed for an additional sample of 5 mice with xenografts of BT474 carcinoma (3+ in the conventional HER2 classification). Estimated initial slopes, characterizing the temporal profile of fluorescence intensities from the tumor after marker injection, were compared to values of HER2 overexpression, obtained by ELISA for the individual mouse after sacrificing the animal. It should be emphasized that the estimates of these initial slopes and the results of ELISA assay of the individual tumors were performed completely independently and then compared. We found that, if we arranged the tumor data points in the order according to the ELISA reading, corresponding slopes would also be arranged in a similar order, ie, from the lowest to the highest one. If compared characteristics (slope, ELISA reading) were not correlated, the probability P of such realization by chance is an inverse of a number of possible permutations, $N = n!|_{n=5} = 120$; i.e., less than 1% (0.83%). Furthermore, Figure 5 shows good linear correlation between both parameters (correlation coefficient $R^2 \cong 0.945$).

Discussion

Analyzing the NIR signal from in vivo experiments presents a complex problem. Strong light scattering in tissues results in inferior resolution of optical imaging for deep tissue abnormalities. Nevertheless, taking into account the known advantages of NIR imaging, several research groups pursue the application of this modality for imaging and quantification of breast abnormalities, located at different depths up to 4–9 cm in breast tissue (e.g. [14,24–28]). The general idea of these efforts is to map optical parameters of the tissue abnormality (e.g., scattering and absorption coefficients—see recent review and references there [29]), and relate the perturbations in optical parameters to variations in physiological status of the tissue, i.e., blood volume/oxygenation. However, up to now the results of optical mammography for characterization of abnormalities have not been sufficiently conclusive to be clinically important. Using a bolus of indocyanine green as a non-targeted absorbing contrast agent allows one to improve the detectability of regions with increased blood volume, but no significant variations in washout kinetics of tumors and healthy breast tissues were observed.

It should be noted that our focus on analysis of signal changes as a function of time, does not involve high-resolution mapping of the ROI and sophisticated 3-D reconstruction algorithms (that up to now have not been successfully realized for clinical studies). While limited in its scope to evaluation of overexpression of specific receptors in the tumor area (ie, in the region with highest fluorescence intensity, originating from specific markers), it is much less sensitive to many uncertainties, characteristic for deep tissue imaging, and can be useful for “optical biopsy” of the tumor *in vivo*, for example, for patient selection or to monitor the response to therapy. Our approach is based on comparison of fluorescent images of the ROI, obtained at subsequent time points after injection of the contrast agent. Under the reasonable assumption that optical properties of the tissue/tumor and imaging geometry are not changed after injection (at least for ~30–70 h. in the considered case of mouse imaging), the attenuation coefficient, related to photon migration in the turbid media, stays the same. Therefore, one can expect that after initial curve normalization at $t = t_1$ (see above) variations in fluorescence intensities due to a specific marker are determined by kinetics of its binding to corresponding receptors and/or its washout from the blood circulation.

Observed correlation between tumor cells HER2 amplification/overexpression and parameters, directly estimated from the sequence of optical images is observed (in particular, initial slope, characterizing the temporal dependence of the fluorescence intensity detected in the tumor) implies that the suggested approach provides a promising tool for *in vivo* characterization of HER2 overexpression in individual tumors.

In conclusion, it should be emphasized that direct quantification of HER2 expression *in vivo*, using maps of absolute fluorescence intensity in the ROI, is impossible due to many complicating factors, such as unknown total blood volume in circulation, dose of fluorescence markers injected, intensity variation with time after injection likely due to changes in fraction of fluorophores, bound to the receptors versus those in the bloodstream, washout of the imaging probe, etc. We believe that only analysis of temporal variations of the fluorescence intensities after injection of the contrast agent, performed in the frames of a compartmental kinetic model (similar to that described above or more sophisticated), can provide quantitative information about HER2 expression in the tumor.

For characterization of tumors, our approach presents an attractive alternative to much more complex schemes of deep tissue optical imaging, such as diffuse optical tomography (which is well known to be a mathematically ill-posed problem), or scanning time-domain optical mammography that can take into account photon migration effects only over very simplifying assumptions, concerning the turbid media (ie., tumor and surrounding tissue).

Though the diffusion effects may be not as significant a factor for our approach as they are for known optical methods for deep-tissue imaging, the transition from the animal model to the clinical studies should require a lot of effort, in particular, to find the proper non-toxic fluorescent marker, design an experimental setup, and develop an adequate kinetic model (similar to that of the mouse, but with different time constants).

Conclusion

Analysis of the temporal profiles of the fluorescent intensities measured in the tumor-associated ROI provided parameters needed to monitor *in vivo* status of the receptors in tumor xenografts characterized by different levels of amplification and expression of HER2.

Acknowledgments

This research is supported by the Intramural Research Program of the National Institute of Child Health and Human Development, and National Cancer Institute, National Institutes of Health, USA.

References

1. Adams GP, Weiner LM. Monoclonal antibody therapy of cancer. Nat Biotechnol. 2005; 23:1147–1157. [PubMed: 16151408]
2. Nahta R, Esteva FJ. Herceptin: mechanisms of action and resistance. Cancer Lett. 2006; 232:123–138. [PubMed: 16458110]
3. Hynes NE, Lane HA. ERBB receptors and cancer: the complexity of targeted inhibitors. Nat Rev Cancer. 2005; 5:341–354. [PubMed: 15864276]
4. Kobayashi H, Shirakawa K, Kawamoto S, et al. Rapid accumulation and internalization of radiolabeled herceptin in an inflammatory breast cancer xenograft with vasculogenic mimicry predicted by the contrast-enhanced dynamic MRI with the macromolecular contrast agent G6-(1B4M-Gd)(256). Cancer Res. 2002; 62:860–866. [PubMed: 11830544]
5. Lub-de Hooge MN, Kosterink JG, Perik PJ, et al. Preclinical characterisation of 111In-DTPA-trastuzumab. Br J Pharmacol. 2004; 143:99–106. [PubMed: 15289297]

6. Milenic DE, Garmestani K, Brady ED, et al. Targeting of HER2 antigen for the treatment of disseminated peritoneal disease. Clin Cancer Res. 2004; 10:7834–7841. [PubMed: 15585615]
7. Smith-Jones PM, Solit DB, Akhurst T, et al. Imaging the pharmacodynamics of HER2 degradation in response to Hsp90 inhibitors. Nat Biotechnol. 2004; 22:701–706. [PubMed: 15133471]
8. Lee SB, Hassan M, Fisher R, et al. Affibody molecules for in vivo characterization of HER2-positive tumors by near-infrared imaging. Clin Cancer Res. 2008; 14:3840–3849. [PubMed: 18559604]
9. Orlova A, Tolmachev V, Pehrson R, et al. Synthetic affibody molecules: a novel class of affinity ligands for molecular imaging of HER2-expressing malignant tumors. Cancer Res. 2007; 67:2178–2186. [PubMed: 17332348]
10. Tolmachev V, Nilsson FY, Widstrom C, et al. 111In-benzyl-DTPA-ZHER2:342, an affibody-based conjugate for in vivo imaging of HER2 expression in malignant tumors. J Nucl Med. 2006; 47:846–853. [PubMed: 16644755]
11. Cheng Z, De Jesus OP, Namavari M, et al. Small-animal PET imaging of human epidermal growth factor receptor type 2 expression with site-specific 18F-labeled protein scaffold molecules. J Nucl Med. 2008; 49:804–813. [PubMed: 18413392]
12. Kramer-Marek G, Kiesewetter DO, Martiniova L, et al. [18F]FBEM-Z(HER2:342)-Affibody molecule-a new molecular tracer for in vivo monitoring of HER2 expression by positron emission tomography. Eur J Nucl Med Mol Imaging. 2008; 35:1008–1018. [PubMed: 18157531]
13. Chen Y, Zheng G, Zhang ZH, et al. Metabolism-enhanced tumor localization by fluorescence imaging: in vivo animal studies. Opt Lett. 2003; 28:2070–2072. [PubMed: 14587818]
14. Rinneberg H, Grosenick D, Moesta KT, et al. Scanning time-domain optical mammography: detection and characterization of breast tumors in vivo. Technol Cancer Res Treat. 2005; 4:483–496. [PubMed: 16173820]
15. Becker A, Hessenius C, Licha K, et al. Receptor-targeted optical imaging of tumors with near-infrared fluorescent ligands. Nat Biotechnol. 2001; 19:327–331. [PubMed: 11283589]
16. Bugaj JE, Achilefu S, Dorshow RB, et al. Novel fluorescent contrast agents for optical imaging of in vivo tumors based on a receptor-targeted dye-peptide conjugate platform. J Biomed Opt. 2001; 6:122–133. [PubMed: 11375721]
17. Engelbrecht CJ, Johnston RS, Seibel EJ, et al. Ultra-compact fiber-optic two-photon microscope for functional fluorescence imaging in vivo. Opt Express. 2008; 16:5556–5564. [PubMed: 18542658]
18. Masotti A, Vicennati P, Boschi F, et al. A novel near-infrared indocyanine dye-polyethylenimine conjugate allows DNA delivery imaging in vivo. Bioconjug Chem. 2008; 19:983–987. [PubMed: 18429627]
19. Mitra S, Foster TH. In vivo confocal fluorescence imaging of the intratumor distribution of the photosensitizer mono-L-aspartylchlorin-e6. Neoplasia. 2008; 10:429–438. [PubMed: 18472960]
20. Hassan M, Riley J, Chernomordik V, et al. Fluorescence lifetime imaging system for in vivo studies. Mol Imaging. 2007; 6:229–236. [PubMed: 17711778]
21. Delforge J, Mesangeau D, Dolle F, et al. In vivo quantification and parametric images of the cardiac beta-adrenergic receptor density. J Nucl Med. 2002; 43:215–226. [PubMed: 11850488]
22. Pegram MD, Konecny GE, O'Callaghan C, et al. Rational combinations of trastuzumab with chemotherapeutic drugs used in the treatment of breast cancer. J Natl Cancer Inst. 2004; 96:739–749. [PubMed: 15150302]
23. Kallioniemi OP, Kallioniemi A, Kurisu W, et al. ERBB2 amplification in breast cancer analyzed by fluorescence in situ hybridization. Proc Natl Acad Sci U S A. 1992; 89:5321–5325. [PubMed: 1351679]
24. Dierkes T, Grosenick D, Moesta KT, et al. Reconstruction of optical properties of phantom and breast lesion in vivo from paraxial scanning data. Phys Med Biol. 2005; 50:2519–2542. [PubMed: 15901952]
25. Grosenick D, Moesta KT, Moller M, et al. Time-domain scanning optical mammography: I. Recording and assessment of mammograms of 154 patients. Phys Med Biol. 2005; 50:2429–2449. [PubMed: 15901947]

26. Grosenick D, Moesta KT, Wabnitz H, et al. Time-domain optical mammography: initial clinical results on detection and characterization of breast tumors. Appl Opt. 2003; 42:3170–3186. [PubMed: 12790468]

27. Grosenick D, Wabnitz H, Moesta KT, et al. Concentration and oxygen saturation of haemoglobin of 50 breast tumours determined by time-domain optical mammography. Phys Med Biol. 2004; 49:1165–1181. [PubMed: 15128196]

28. Ntziachristos V, Yodh AG, Schnall M, et al. Concurrent MRI and diffuse optical tomography of breast after indocyanine green enhancement. Proc Natl Acad Sci U S A. 2000; 97:2767–2772. [PubMed: 10706610]

29. Rinneberg H, Grosenick D, Moesta KT, et al. Detection and characterization of breast tumours by time-domain scanning optical mammography. Opto-Electronics Review. 2008; 16:147–162.

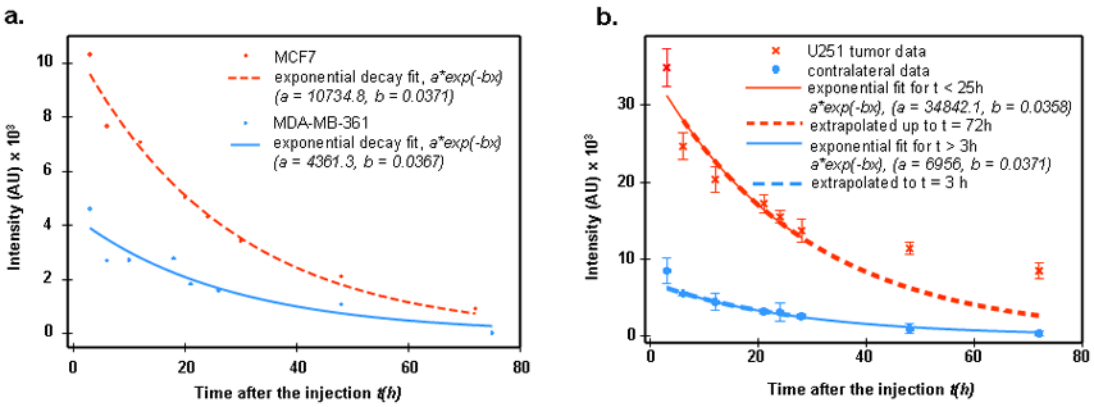

Figure 1.

Figure 1a. Exponential decay *a exp(−bt)* fit to contralateral data for MCF7 and MDA-MB361 cases.

b. U251 tumor and contralateral data (after background subtraction) (residual values for long times t = 48, 72 hours I1, 2 = 5140, 5828, respectively).

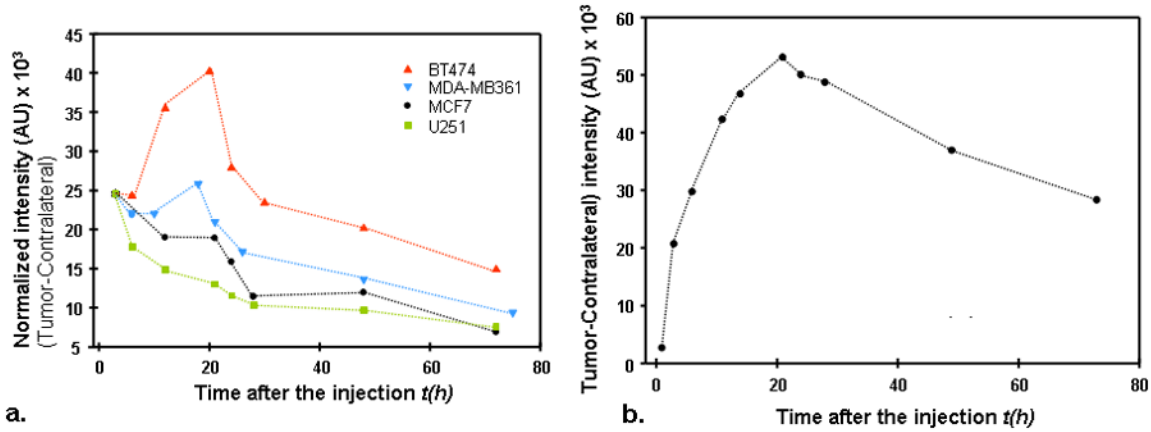

Figure 2.

Figure 2a. Difference between normalized tumor–contralateral data, as a function of time, for four tumor types, differing in HER2 expression.

b. Difference between normalized tumor–contralateral data (BT474 xenograft), measured at shorter time intervals in the first 25 hours for one of the mice in the second series of measurements.

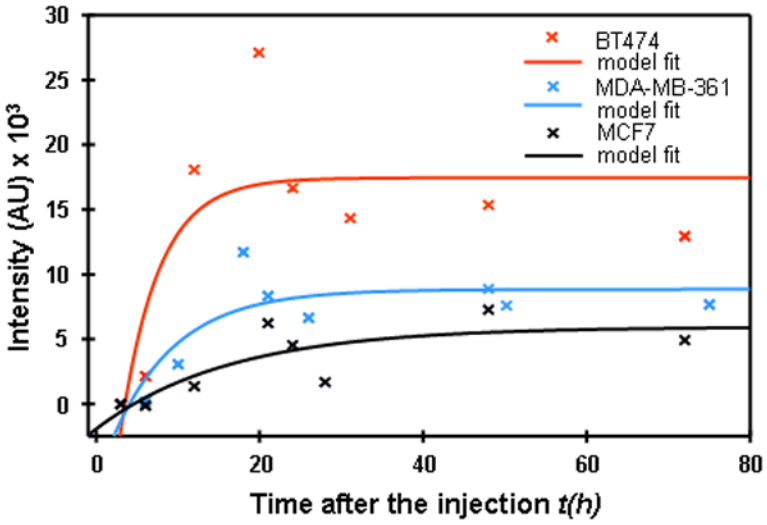

Figure 3.
Fitting of normalized tumor–contralateral data by a function $y=y_0+a*(1-exp(-bx))$.

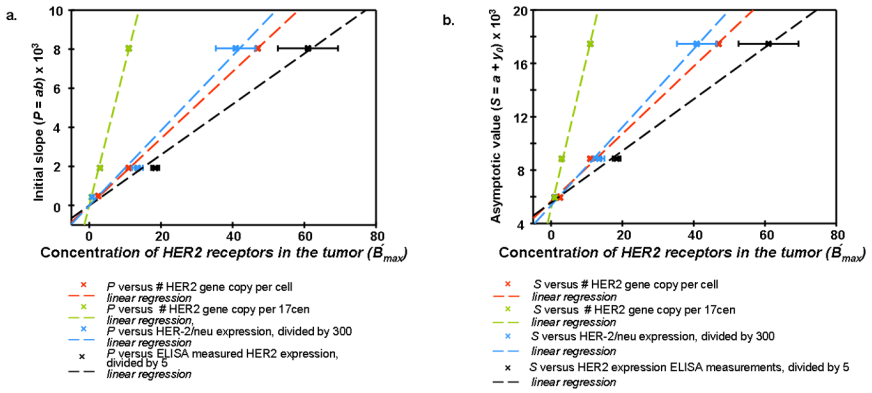

Figure 4.

Figure 4a. Correlation between parameter *P=ab* (intial slope) in the Exponential Regression and quantitative characteristics of amplification and overexpression of HER2 for breast carcinoma cell lines MCF7, MDA-MB361, BT474.

b. Correlation between parameter *S=y0+a* (asymptotic intensity) in the Exponential Regression and quantitative characteristics of amplification and overexpression of HER2 for breast carcinoma cell lines MCF7, MDA-MB361, BT474.

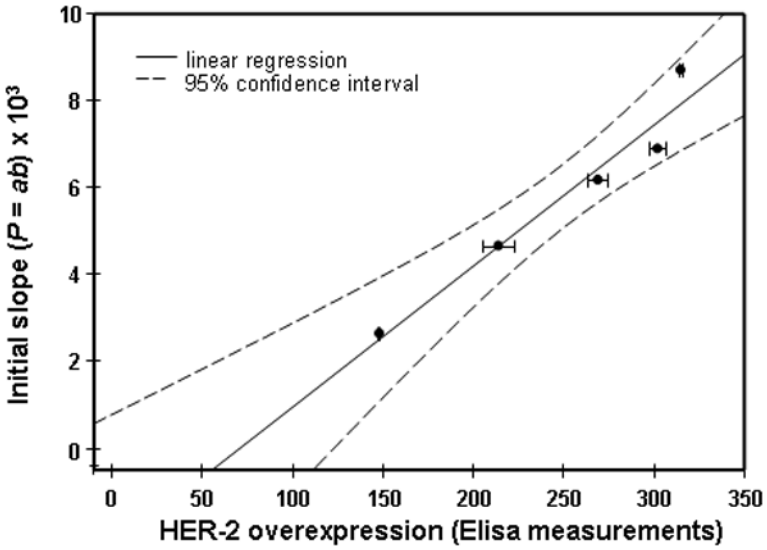

Figure 5.

Correlation between parameter *P=ab* (intial slope) in the Exponential Regression and overexpression of HER2 for breast carcinoma cell BT474, measured by ELISA *ex vivo* assay after optical imaging of the same mouse at different time points *in vivo.*

Table 1

Difference in intensities between tumor and contralateral site data for each tumor category (data averaged over each subsample).

BT474		U251		MCF7		MDA-MB361	
Time	**Tumor - Contralateral**	**Time**	**Tumor - Contralateral**	**Time**	**Tumor - Contralateral**	**Time**	**Tumor - Contralateral**
3	24535.2	3	24015.0	3	19946.0	3	9050.4
6	24102.4	6	16740.0	6	17754.1	6	8170.9
12	35452.2	12	13558.0	12	15421.2	10	8119.3
20	40181.8	21	11604.0	21	15331.3	18	9523.4
24	27879.1	24	9991.0	24	12869.5	21	7725.6
30	23401.0	28	8683.5	28	9282.6	26	6325.3
48	20140.1	48	8053.0	48	9693.2	48	5026.2
72	14879.0	72	5736.2	72	5573.1	75	3464.6

Mol Imaging. Author manuscript; available in PMC 2012 July 23.

Table 2

Parameters, initial slope $P = ab$ and asymptotic intensity $S = y_0 + a$, extracted from the fit of experimental data for 3 tumor types to the theoretical model $y = y_0 + a(1-e^{-bx})$ (see Figure 3)

Tumor type	*P*	*S*
BT474	8043.6	17465.0
MDA-MB361	1921.6	8858.0
MCF7	481.2	5948.7

Table 3

Parameters of the linear regression $y = b^1 + b^1 x$, characterizing correlation between amplification/overexpression of HER2 and values of initial slope P and intensity S, obtained from data in Figure 4a and b

	P		S	
	b[0]	b[1]	b[0]	b[1]
No. of HER2 gene copy per cell	0	171.4	5855.0	248.1
No. of HER2 gene copy per 17 cen	0	723.0	5318.1	1108.2
No. of HER2/neu expression (divided by 300)	0	191.7	5353.1	293.1
Her2 expression, ELISA measured (divided by 5)	0	129.7	5559.7	193.9